

# The two Janus faces of CpRu-based deallylation catalysts and their application for *in cellulo* prodrug uncaging.

Alain Baiyoumy,<sup>Δ</sup> Robin Vinck,<sup>Δ</sup> Thomas R.Ward\*<sup>Δ</sup>

<sup>Δ</sup> Department of Chemistry, University of Basel, 4058 Basel, Switzerland; Molecular SystemsEngineering, National Competence Center in Research (NCCR), 4058 Basel, Switzerland

## Corresponding Author:

Thomas R. Ward; orcid.org/0000-0001-8602-5468; Email: thomas.ward@unibas.ch

## Authors:

Alain Baiyoumy; orcid.org/0000-0003-3007-4724

Robin Vinck; orcid.org/0000-0002-2730-0121

## Acknowledgment:

The authors thank Pascal Rieder and Daniel Haussinger for their help with NMR experiments. The authors thank Jonas Zurflüh for his help with analytical instrumentation. The authors thank Michael Pfeffer for his precious help with the MS experiments. T.R.W. acknowledges the Swiss National Science Foundation (Grant 200020\_182046) as well as the NCCR Molecular Systems Engineering for funding.

## Notes:

The authors declare no competing financial interest.

## Author contribution

AB conceived the project, performed all *in vitro* experiments, developed the analytical methods, and wrote the manuscript with input from RV and TRW. RV carried out all the *in-cellulo* experiments and the associated analytics and revised the manuscript. TRW conceived and supervised the project and revised the manuscript.

## Abstract

In the past 16 years, metal-catalyzed deallylation has proven a useful tool for studying biological processes *in cellulo* and in the early development of innovative therapeutic catalytic strategies. This reaction is catalyzed by Ru-piano stool complexes and has been reported to be compatible with air, water, and thiol-containing compounds such as glutathione. However, little is known about the true influence of biological components on the outcome of this reaction. The results presented herein reveal that the co-solvent used in this reaction affects the complex's stability and activity in air, while the presence of glutathione contributes to minimizing the formation of *N*-allylated by-products. In addition, we studied the effect of air on the Ru-catalyzed deallylation. Importantly, we found that, in the presence of air, the complex is deactivated and oxidizes glutathione into its disulfide.

## Introduction

In 2006, Meggers and co-workers reported that  $[\text{Cp}^*\text{Ru}^{\text{II}}(\text{cod})\text{Cl}]$  ( $\text{Cp}^*$  = cyclopentadienyl and  $\text{cod}$  = 1,5-cyclooctadiene) catalyzes the deprotection of alloc-protected amines in the presence of thiols and air.<sup>1</sup> In 2014, they used  $[\text{CpRu}^{\text{II}}(\text{NMe}_2\text{-QA})(\text{solv})]$  **1** (QA = quinaldic acid,  $\text{solv}$  = solvent) **1** and  $[\text{CpRu}^{\text{IV}}(\text{NMe}_2\text{-QA})(\eta^3\text{-allyl})]^+$  **2** for the same reaction and proposed a possible catalytic cycle, Figure 1.<sup>2</sup>

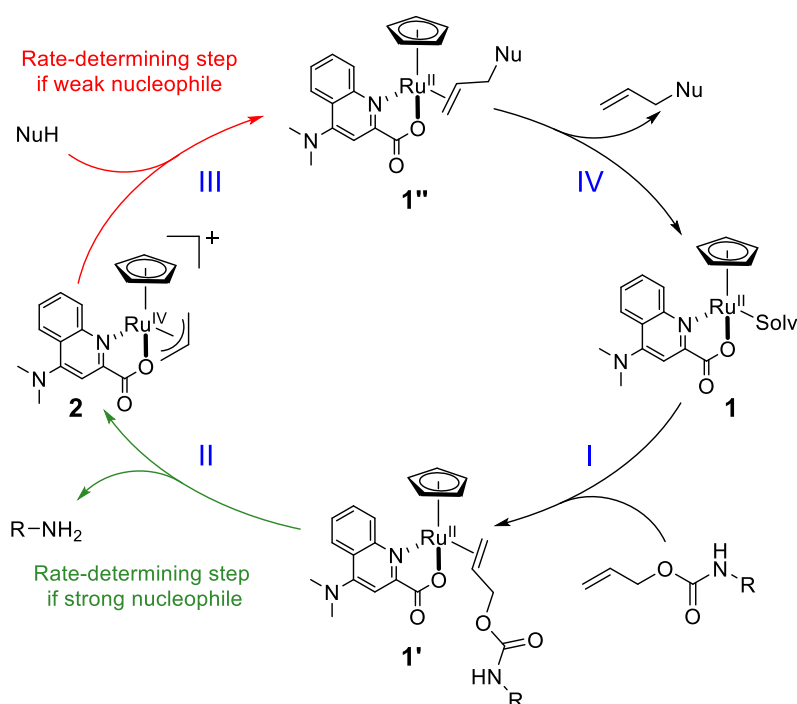


**Figure 1:** Proposed mechanism for the Ru-catalyzed deallylation of alloc-protected amines. **I**] Coordination of the alloc-protected amine to **1**. **II**] Oxidative ligand transfer of the allyl moiety to the Ru(II)-center, affording the {Ru(IV)(η<sup>3</sup>-allyl)}-complex **2** and the uncaged amine R-NH<sub>2</sub>. **III**] Nucleophilic addition on the η<sup>3</sup>-allyl resulting in the {Ru(II)(η<sup>2</sup>-alkene)}-complex **1''**. **IV**] Regeneration of the [CpRu<sup>II</sup>(NMe<sub>2</sub>-QA)(solv)] **1** by alkene-displacement with the solvent (solv). Adapted from Meggers and co-workers.<sup>2</sup>

In a related study, Kitamura and co-workers investigated how the substituent on the bidentate ligand affects the activity of the catalyst in methanol and dichloromethane and found that electron-withdrawing groups have a beneficial effect.<sup>3</sup> In contrast, Meggers and co-workers reported that electron-donating groups on the ligand lead to an increased activity in aqueous media. This difference may be caused by the different substrates (i.e. electron-rich for Kitamura and co-workers, electron-poor for Meggers and co-workers) used in these studies as well as the bidentate ligand itself (i.e. pyridine-based for Kitamura and co-workers, quinoline-based for Meggers and co-workers).<sup>2</sup>

While thiols are generally poisonous to soft-metal-based catalysts, the CpRu-based deallylation catalysts reported by Meggers and co-workers were shown to maintain their activity *in cellulo*. Despite the presence of millimolar concentrations of reduced glutathione (GSH hereafter) in the cytoplasm of aerobic cells,<sup>2,4-12</sup> they reported the intracellular functionalization of  $\eta^3$ -allyls with nucleophilic thiols using these catalysts in a few instances.<sup>13,14</sup> This inspired multiple studies, whereby derivatives of catalysts **1** or **2** were used to uncage a variety of alloc-protected cargoes *in cellulo*, including fluorophores, drugs, hormones, amino acids, etc.<sup>4,5,7-12,15-24</sup>

In 2010, Waymouth and co-workers further investigated the catalyst's behavior in the presence of organic solvent and oxygen.<sup>15</sup> They found that the reaction did not proceed to completion in the presence of oxygen, suggesting a possible competition between two reactions: oxidative degradation of the catalyst vs. deallylation. Further, Wender and co-workers observed a side reaction caused by the nucleophilic nature of the uncaged amine.<sup>16</sup> Indeed, the uncaged primary amine may act as a (parasitic) nucleophile, which attacks the  $\eta^2$ -alkene to afford the corresponding (di)-allylated amine.

The third generation Ru(II)-based catalyst  $[\text{CpRu}^{\text{IV}}(\text{HQ})(\eta^3\text{-allyl})]^+$  **3** was reported by Meggers in 2017 and used for the uncaging of *N*-alloc-protected cargoes *in cellulo*.<sup>6</sup> However, its improved catalytic performance vs. complex **1** in biological media has been a matter of debate.<sup>20,26</sup> Importantly,  $[\text{CpRu}^{\text{IV}}(\text{HQ})(\eta^3\text{-allyl})]^+$  complexes have been reported to be cytotoxic *in vivo*.<sup>17,18</sup>

In this study, we set out to investigate how the presence of GSH, O<sub>2</sub>, and the nature of the co-solvent affect the activity and the stability of  $[\text{CpRu}^{\text{II}}(\text{NMe}_2\text{-QA})(\text{solv})]$  **1**, using the coumarin derivative **5** as substrate.

## Results and Discussion

It has been observed, both in our lab and elsewhere, that the presence of air affects Ru-catalyzed reactions involving  $\eta^3$ -allyl precursors.<sup>15,17-19</sup> Moreover, a pronounced effect of the organic co-solvents on the complex's activity and stability in the presence of air has been reported.<sup>17</sup> To investigate this further, we measured a set of <sup>1</sup>H NMR spectra of  $[\text{CpRu}^{\text{II}}(\text{NMe}_2\text{-QA})(\text{solv})]$  **1** in the presence/absence of air, using different organic co-solvents. The resulting <sup>1</sup>H NMR spectra highlight a marked influence of the solvent on the stability of  $[\text{CpRu}^{\text{II}}(\text{NMe}_2\text{-QA})(\text{solv})]$  **1**, Figure 2.

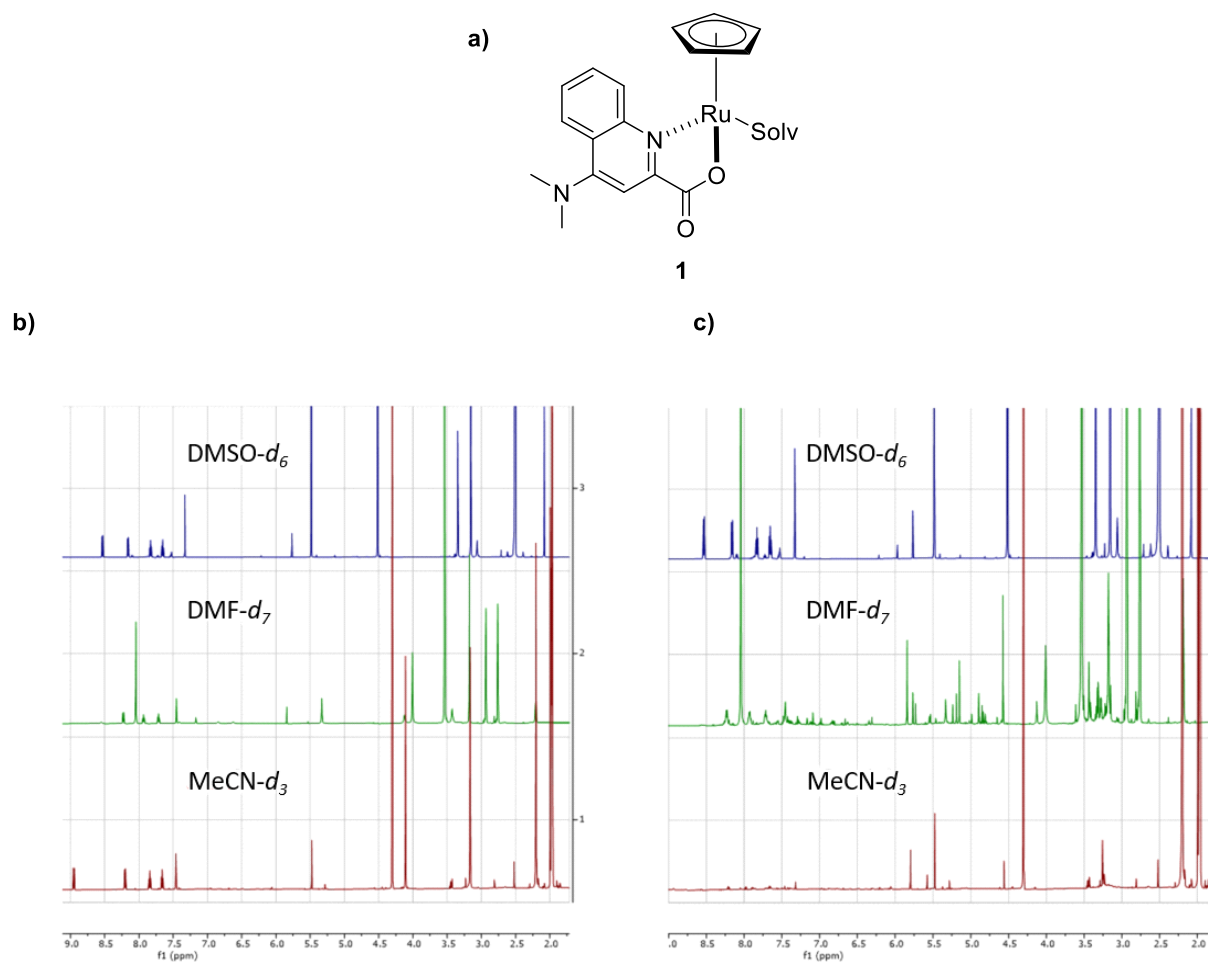


**Figure 2:**  $^1\text{H}$  NMR spectra of catalyst **1** recorded in different deuterated solvents: a) structure of catalyst **1**. b)  $^1\text{H}$  NMR recorded in the absence of air. c)  $^1\text{H}$  NMR recorded following 15 min exposure to air. The degradation of the catalyst can be observed in MeCN and DMF but not in DMSO.

As can be appreciated in Figure 2 b-c, the organic solvent has a pronounced effect on the stability of complex **1** towards air. Strikingly, DMSO protects  $[\text{CpRu}^{\text{II}}(\text{NMe}_2\text{-QA})(\text{solv})]$  **1** from aerobic degradation, raising the question of the involvement of the solvent in affecting the catalyst's stability against air.

According to Meggers, the Ru-based catalytic deallylation reaction is more efficient in the presence of thiols, which act as strong nucleophiles (i.e. thiophenol or GSH) towards the  $\eta^3$ -allyl.<sup>2,6</sup> This finding sparked our interest since thiols, such as reduced glutathione

(GSH), are present in high concentrations in intracellular environments and have thus far impeded our own work on intracellular catalysis using artificial metalloenzymes.<sup>5</sup> We thus set out to probe the mechanistic involvement of thiols, specifically glutathione, in more detail.

First, the stability of  $[\text{CpRu}^{\text{II}}(\text{NMe}_2\text{-QA})(\text{solv})]$  **1** towards the GSH was evaluated. For this purpose, we recorded its  $^1\text{H}$  NMR spectrum in  $\text{D}_2\text{O}$  and added GSH (100 eq. vs. **1**) in the presence/absence of air. While no significant change was observed in the  $^1\text{H}$  NMR spectrum in the absence of air, the oxidized form of GSH, glutathione disulfide (GSSG), was detected in the presence of air, Figure 3. Since  $^3\text{O}_2$  does not oxidize GSH in the absence of a catalyst/enzyme, we conclude that the reaction is catalyzed by  $[\text{CpRu}^{\text{II}}(\text{NMe}_2\text{-QA})(\text{solv})]$  **1** (see Supporting Information).

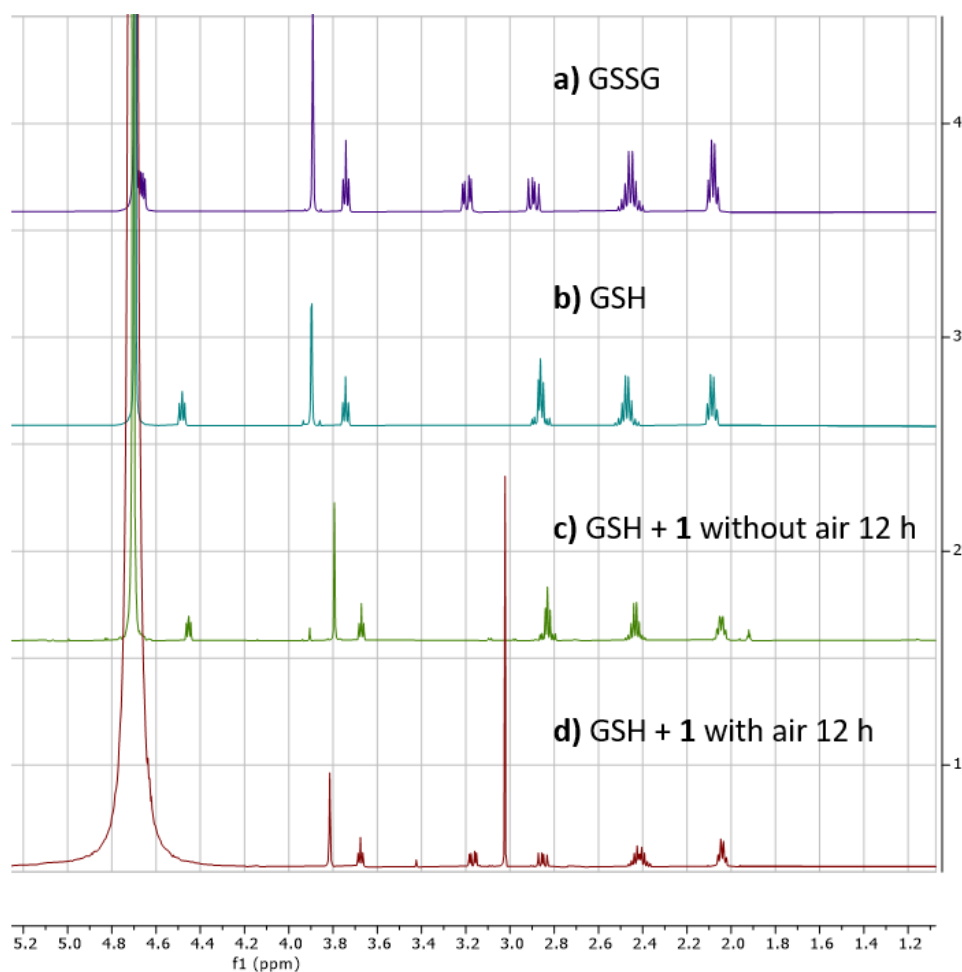


**Figure 3:**  $^1\text{H}$  NMR-monitoring of the  $[\text{CpRu}^{\text{II}}(\text{NMe}_2\text{-QA})(\text{solv})]$  **1**-catalyzed GSH oxidation by air. a)  $^1\text{H}$  NMR spectrum of GSSG in  $\text{D}_2\text{O}$ , b)  $^1\text{H}$  NMR spectrum of GSH in  $\text{D}_2\text{O}$ , c)  $^1\text{H}$  NMR spectrum of GSH + 5 mol% **1** in  $\text{D}_2\text{O}$  without exposure to  $\text{O}_2$ , and d)  $^1\text{H}$  NMR spectrum of GSH + 5 mol% **1** in  $\text{D}_2\text{O}$  after exposure to  $\text{O}_2$ . The signal at 3.02 ppm corresponds to dimethylsulfone (added as internal standard in d). Sample preparation:  $\text{D}_2\text{O}$  (475  $\mu\text{L}$ ), GSH (20  $\mu\text{L}$  of 50 mM stock solution in water), and  $[\text{CpRu}^{\text{II}}(\text{NMe}_2\text{-QA})(\text{solv})]$  **1** (5  $\mu\text{L}$  of a 10 mM stock solution in MeCN) (total volume 500  $\mu\text{L}$ ) were mixed under inert conditions. Subsequently, dimethylsulfone (100  $\mu\text{L}$ , 6 mM stock) was added to the tube as an NMR standard for quantification (in d)).

These results unambiguously reveal that GSH is oxidized into GSSG in the presence of  $[\text{CpRu}^{\text{II}}(\text{NMe}_2\text{-QA})(\text{solv})]$  **1** and air. If the complex itself does indeed catalyse the oxidation of GSH *in cellulo*, its use could be potentiated by combining the uncaging of cytotoxic drugs with the oxidation of GSH.<sup>20</sup> Indeed, it has been shown that the oxidation of GSH to GSSG affects the redox balance of the cell, eventually leading to cell death.<sup>21</sup>



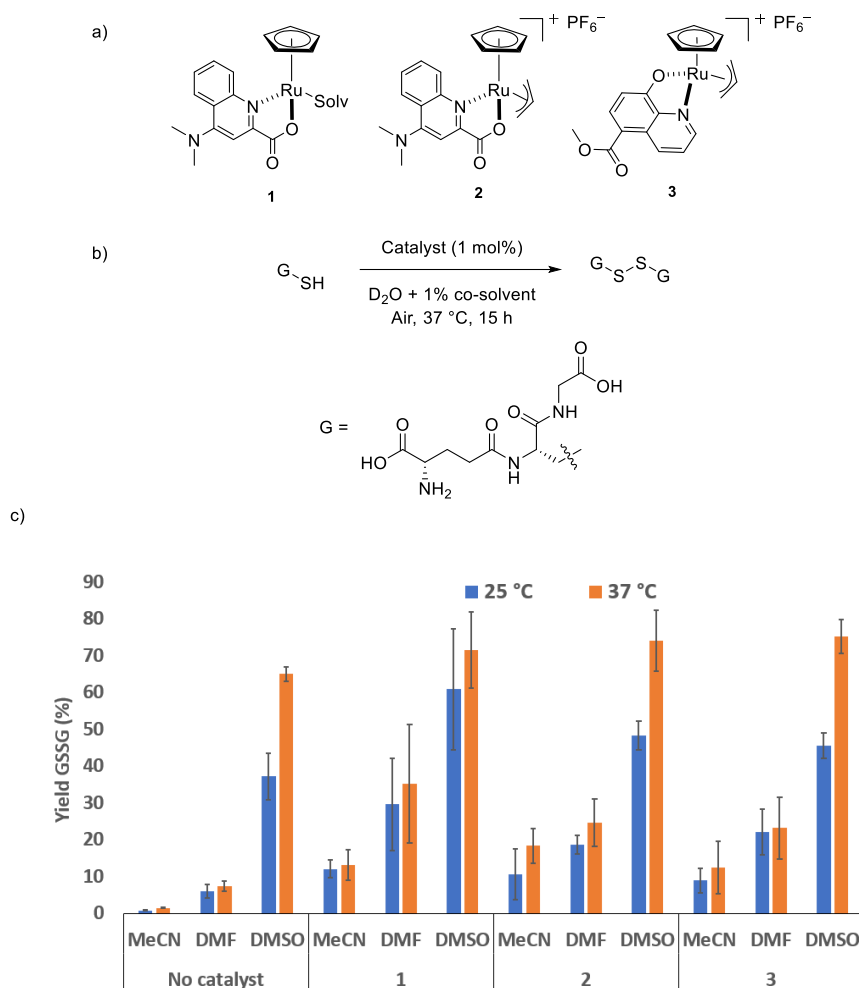
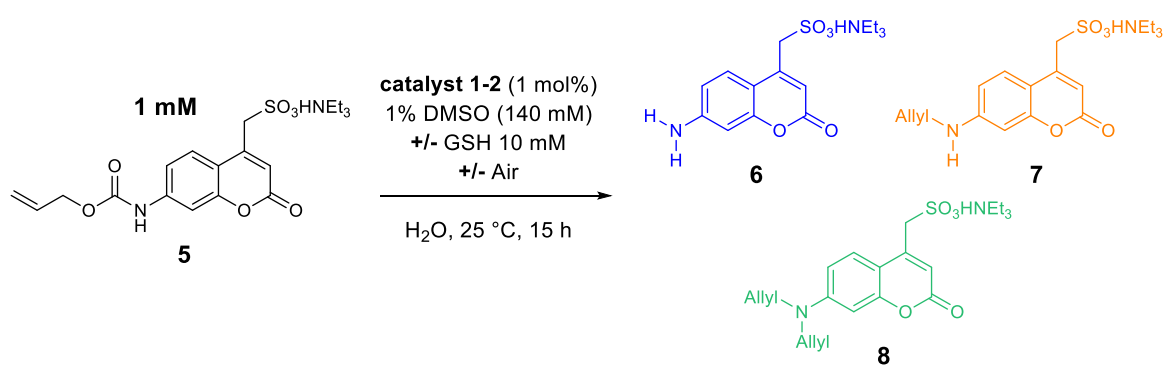


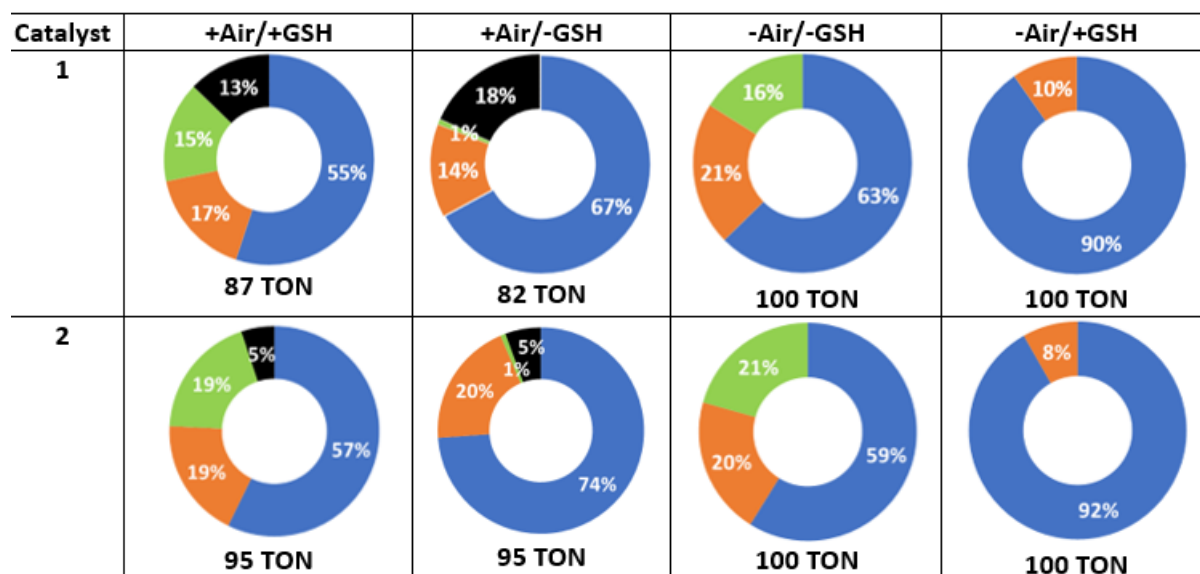
**Figure 4:** Catalytic aerobic oxidation of glutathione by CpRu catalysts **1-3**, monitored by  $^1\text{H}$  NMR. The reactions were performed in an open flask in the presence of air. Sample preparation:  $\text{D}_2\text{O}$  (395  $\mu\text{L}$ ), GSH (100  $\mu\text{L}$  of 50 mM stock solution in water), and catalyst **1-3** (5  $\mu\text{L}$  of a 10 mM stock solution in the corresponding solvent) (total volume 500  $\mu\text{L}$ ) were mixed in inert conditions. Subsequently, dimethylsulfone (100  $\mu\text{L}$ , 6 mM stock) was added to the tube as an NMR standard for quantification

However, for this added feature to be practical, the GSH oxidation reaction should be catalytic. To investigate this further, the amount of GSH oxidized to GSSG was quantified in the presence of catalysts **1-3** and air in different solvents, Figure 4. The results indicate that the reaction is indeed catalytic, which may contribute further to the cytotoxicity of the deallylation catalysts **1-3**. Further, the Ru-catalyzed oxidation of GSH may minimize

the detrimental effect of GSH on the soft metal center, contributing to its activity in a cellular environment. Strikingly, the yield of oxidized products was much higher in DMSO than in DMF and MeCN. In DMSO, GSH is oxidized even in the absence of a catalyst, a feature that has been previously reported in the presence of air by Walker and co-workers.<sup>22</sup> To minimize the possibility that trace contaminants in the commercial DMSO are responsible for the oxidation reaction, we performed the reaction with DMSO purchased from five different vendors, Figure S11.

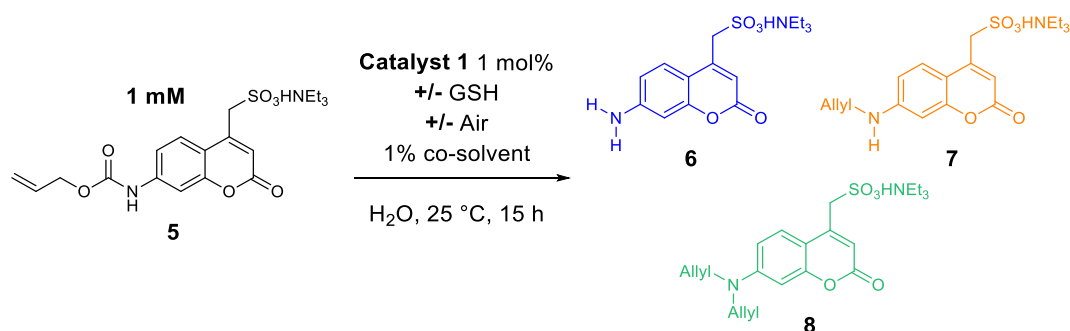
Next, the Ru-catalyzed deallylation of the alloc-protected coumarin **5** was selected as a test reaction to scrutinize the influence of dioxygen and GSH on the reaction, using [CpRu<sup>II</sup>(NMe<sub>2</sub>-QA)(solv)] **1** and [CpRu<sup>II</sup>(NMe<sub>2</sub>-QA)(Allyl)]PF<sub>6</sub> **2** as catalysts. As the vast majority of *in cellulo* studies with CpRu-based catalysts use DMSO as co-solvent, we also selected this non-innocent solvent for this study. Under these reaction conditions, we anticipate that a significant fraction of the GSH will be present in its oxidized form GSSG, see Figures 4-5.





**Figure 5:** Deallylation of the alloc-protected coumarin **5** with catalysts [CpRu<sup>II</sup>(NMe<sub>2</sub>-QA)(solv)] **1** or [CpRu<sup>II</sup>(NMe<sub>2</sub>-QA)(Allyl)]PF<sub>6</sub> **2** in water containing 1% DMSO and color-coded distribution of the aminocoumarin products **6-8**.

The following trends can be gathered from these experiments: i) Neither GSH nor air significantly affect the overall catalytic performance, as reflected by the total turnover number. ii) The catalytic performance of CpRu-complexes **1** and **2** is similar. This is anticipated, as both are part of the deallylation catalytic cycle (Figure 1). iii) The presence of GSH does affect the product distribution (e.g., coumarin **6** vs. monoallyl-coumarin **7** vs. diallyl coumarin **8**) to some extent. As GSH competes with the aniline moiety of coumarin **6** in the nucleophilic substitution step of the catalytic cycle (Figure 1, step III), its presence minimizes the formation of the undesired allylated coumarins **7-8**.



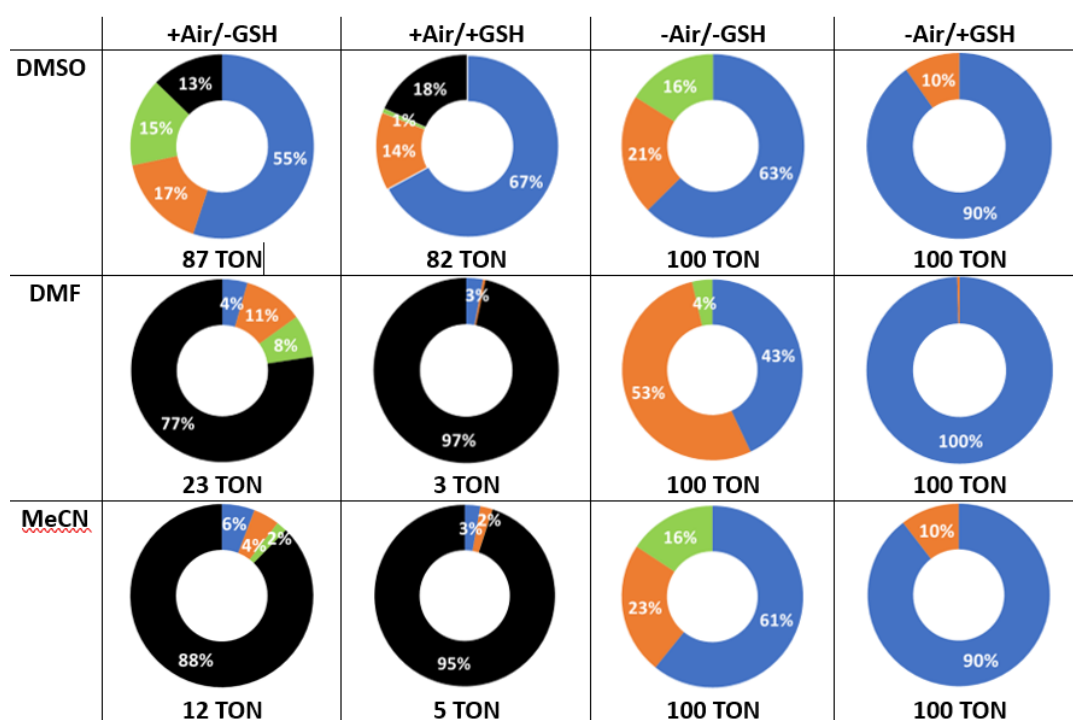
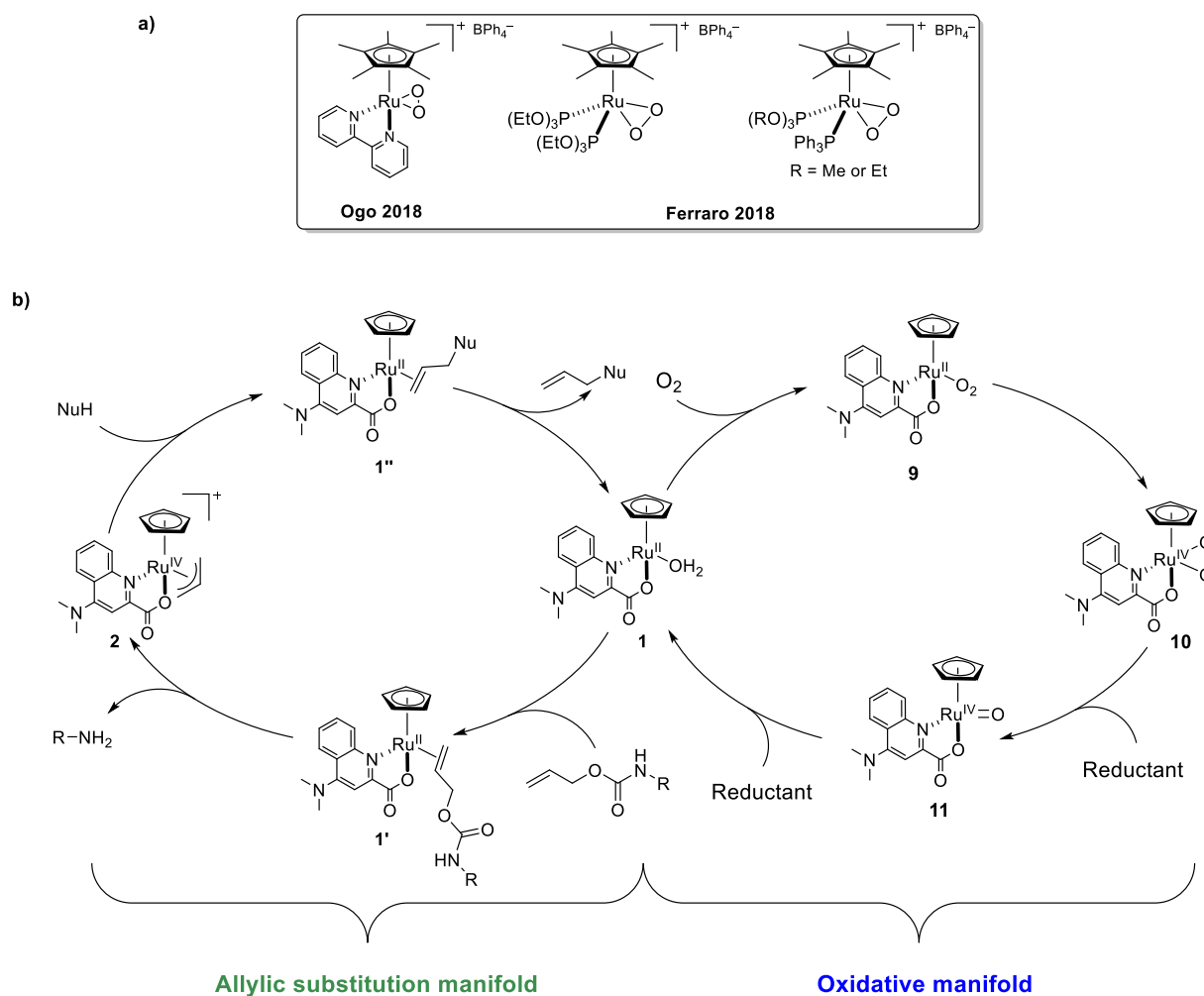


**Figure 6:** Product distribution resulting from the deallylation reaction in different co-solvents. The total turnover number (TON) and color-coded product distribution are displayed.

However, as the presence of DMSO positively affects the catalyst's stability (Figure 2), we tested the influence of DMF and MeCN on the catalytic activity of  $[\text{CpRu}^{\text{II}}(\text{NMe}_2\text{-QA})(\text{solv})]$  **1**, Figure 6 and Table S2. Thereby, the following trends emerged: i) In stark contrast to the experiments performed with 1% DMSO as co-solvent, the catalytic performance of  $[\text{CpRu}^{\text{II}}(\text{NMe}_2\text{-QA})(\text{solv})]$  **1** in DMF and MeCN is dramatically affected by the presence of air. Hence, under aerobic conditions, DMSO should preferentially be used as a co-solvent in catalysis. ii) In the absence of dioxygen, the effect of GSH on the total turnover number (TON) is negligible for all co-solvents studied but positively affects the selectivity. iii) In the presence of dioxygen, GSH positively affects the product distribution, favouring the formation of the desired aminocoumarin product **6**. Nevertheless, GSH does not affect the

conversion to the desired product **6** when DMSO is used as co-solvent, but markedly decreases it when MeCN or DMF are used as co-solvent.

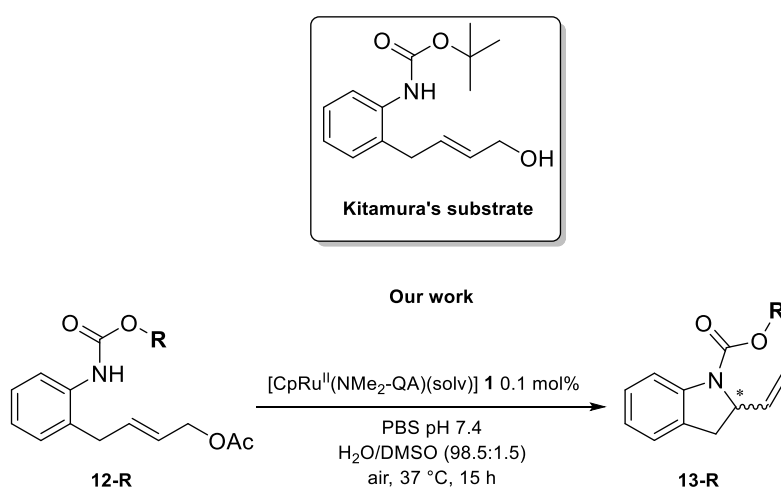
In 2018, Ogo and Ferraro examined several [Cp\*Ru]-based complexes and their reactivity towards O<sub>2</sub>, Figure 7a.<sup>23,24</sup> These studies led them to conclude that, in the presence of O<sub>2</sub>, [Cp\*Ru<sup>IV</sup>]-peroxo complexes are formed, which catalyze the oxidation of phosphite, phosphine, and guanosine-5'-monophosphate (GMP).<sup>23,24</sup> Based on these findings, we propose two competing catalytic manifolds to rationalize the combined aerobic catalytic activity of [CpRu<sup>II</sup>(NMe<sub>2</sub>-QA)(solv)] **1** towards GSH and alloc-protected coumarin **5**, Figure 7b.



**Figure 7:** The Janus-faced catalytic activity of {Cp\*RuL<sub>2</sub>}-complexes. a) Structure of the [Cp\*Ru(IV)L<sub>2</sub>(O<sub>2</sub>)]-complexes reported by Ogo and Ferraro. b) Proposed two catalytic manifolds revolving around [CpRu<sup>II</sup>(NMe<sub>2</sub>-QA)(solv)] **1**.

Inspired by the reports of Ogo and Ferraro, we hypothesize that dioxygen reacts with [CpRu<sup>II</sup>(NMe<sub>2</sub>-QA)(solv)] **1** to afford the corresponding [CpRu<sup>IV</sup>(NMe<sub>2</sub>-QA)(η<sup>2</sup>-O<sub>2</sub>)] **9**. Using the well-established horseradish peroxidase assay, we tested for the presence of H<sub>2</sub>O<sub>2</sub>, but no hydrogen peroxide was detected, Figure S12-14. We thus hypothesize that two equivalents of GSH act as reductant to regenerate the catalytically-competent [CpRu<sup>II</sup>(NMe<sub>2</sub>-QA)(solv)] **1**, which can engage in the deallylation catalytic manifold. {Ru(IV)=O}-species have been investigated towards their oxygenase activity.<sup>25</sup> As illustrated in Figure 7, the negative effect of dioxygen on the deallylation performance in either DMF or MeCN can be partially compensated for by the presence of GSH. Here, the thiol serves a dual function: i) it acts as nucleophile toward the {Ru<sup>IV</sup>(η<sup>3</sup>-allyl)}-moiety in the allylic-substitution manifold, and ii) it converts {Ru<sup>IV</sup>(η<sup>2</sup>-O<sub>2</sub>)} back to the catalytically-competent [CpRu<sup>II</sup>(NMe<sub>2</sub>-QA)(solv)] **1** via the oxidative manifold, thereby oxidizing GSH and thus minimizing its detrimental effect on the catalyst. In contrast to experiments carried out in either DMF or MeCN, the presence of the strongly coordinating DMSO co-solvent has two beneficial effects: i) The coordination of O<sub>2</sub> is minimized, and ii) a yet-to-be-identified decomposition pathway revealed by <sup>1</sup>H NMR for other solvents (see Figure 2) is minimized. The combined beneficial effects of DMSO result in increased deallylase activity. These features, combined with the oxidation potential of DMSO towards GSH, provide a significant advantage in the use of DMSO as a co-solvent for *in vivo* deallylation experiments, Figure 4.

For almost a decade,  $[\text{CpRu}^{\text{II}}(\text{NMe}_2\text{-QA})(\text{solv})]$  derivatives and, more recently,  $[\text{CpRu}^{\text{IV}}(\text{HQ})(\eta^3\text{-allyl})]$  derivatives, were used to catalyze deallylation reactions for *in cellulo* purposes. To increase the versatility of this allylic substitution *in cellulo*, we set out to adapt the allylic amination reaction described in 2012 by Kitamura to physiological conditions.<sup>26</sup> The reaction was initially reported by Kitamura using a mixture of *t*-BuOH/DMA (10:1) with 0.1% catalyst loading in the absence of air at 100 °C.<sup>26</sup> Instead, we used a PBS buffer (pH = 7.4 at 37 °C). Initial attempts revealed substantial limitations due to the presence of air. We hypothesize that the size of the alkyl group on the nucleophilic carbamate might negatively affect its nucleophilicity and set out to investigate if this effect could be counteracted by using smaller substituents, Figure 8. For comparison purposes, the alloc-coumarin substrate **5** was included in this study, Figure 8.



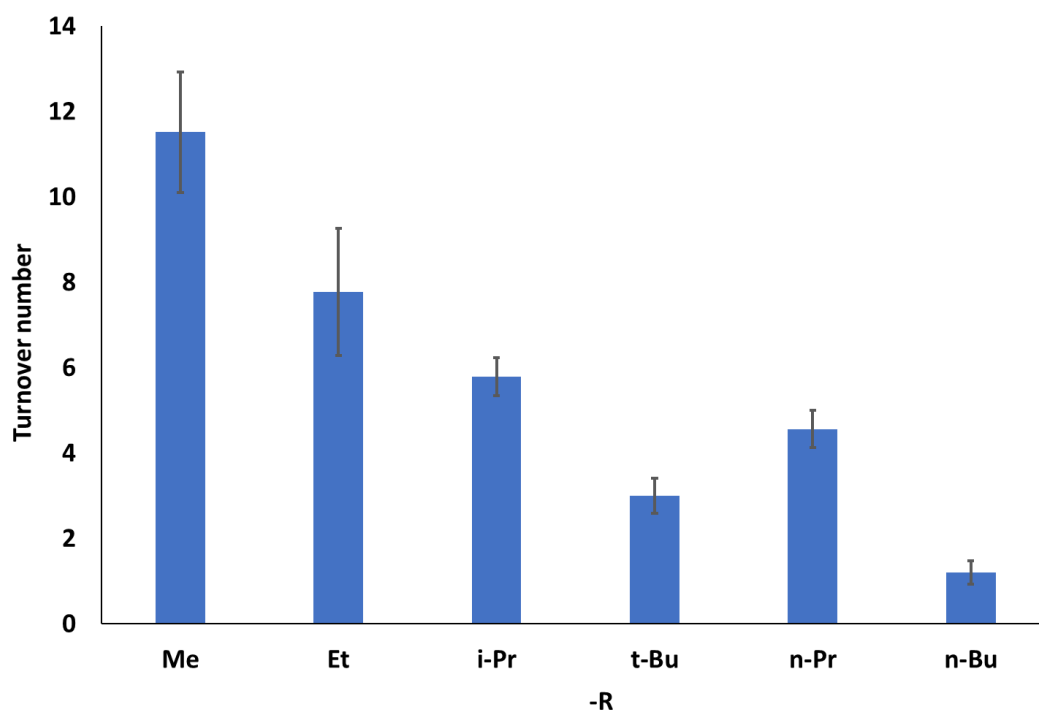


**Figure 8:** Impact of the steric bulk of the urea nucleophile on the ruthenium-catalyzed allylic amination reaction in the presence of substrate **12-R**. The TONs were determined by HPLC. For comparison, under identical reaction conditions, the intermolecular allylic substitution using alloc-protected coumarin **5** yields coumarin **6** with > 120 TON.

Strikingly, the observed TONs for the intramolecular allylic substitution of the substrates **12-R** are markedly lower than for the intermolecular deallylation of aminocoumarin **5** under identical conditions: 11.5 TON for **13-Me** vs. > 120 for substrate **5**. However, no deacetylated side product was observed (addition of water on the  $\pi$ -allyl intermediate). This suggests that the nucleophilicity of the carbamate moiety is the cause of the decreased TON. As the bulkiness of the carbamate-substituent has a modest influence on the TON, we surmise that the limited accessibility of the allyl moiety for coordination to the Ru center affects the activity of the catalyst (i.e., favoring the coordination of O<sub>2</sub> vs. allyl, Figure 7b). For *in cellulo* catalytic applications, an accessible terminal allyl moiety should thus be used.



One of the most enticing applications for the CpRu-based deallylation catalysts **1-3** is their use to uncage *in vivo* cytotoxic drugs via deallylation.<sup>6</sup> To do so, it is crucial to accumulate the catalyst in the cytosol of cancer cells. Essential features of such catalysts should include: i) non-toxicity, ii) efficient uncaging of prodrugs in the presence of oxygen as well as all metabolites present either in the extracellular medium or the cytosol, and iii) maintaining a high catalytic activity at low concentrations (i.e., < 5  $\mu$ M). Meggers and co-workers reported that the analogs of [CpRu<sup>IV</sup>(HQ)( $\eta^3$ -allyl)] **3** were up to 10 times more active than the analogs of [CpRu<sup>IV</sup>(NMe<sub>2</sub>-QA)( $\eta^3$ -allyl)] **2** at uncaging alloc-protected amines in biological media.<sup>6</sup> Building on these findings, Mao and co-workers uncaged an alloc-protected gemcitabine prodrug in a zebrafish embryo xenograft model.<sup>27</sup> Importantly, however, [CpRu<sup>IV</sup>(HQ)( $\eta^3$ -allyl)] **3** was also found to be highly cytotoxic in HeLa cells, with an IC<sub>50</sub> of 70 nM.<sup>22</sup> One may hypothesize that the catalytic activity of [CpRu<sup>IV</sup>(HQ)( $\eta^3$ -allyl)] **3** could be potentiated by its cytotoxicity. To test this hypothesis, we set out to compare the cytotoxicity of [CpRu<sup>IV</sup>(NMe<sub>2</sub>-QA)( $\eta^3$ -allyl)] **2** and [CpRu<sup>IV</sup>(HQ)( $\eta^3$ -allyl)] **3** in CT26 cells (mouse colon carcinoma cell line). For this purpose, we adapted the reaction conditions from the publication by Meggers and co-workers<sup>6</sup> and performed the experiments with CT26 cells in the presence of air and 0.5 % v/v of DMSO. As displayed in Figure 9a, [CpRu<sup>IV</sup>(HQ)( $\eta^3$ -allyl)] **3** is only slightly more cytotoxic than [CpRu<sup>IV</sup>(NMe<sub>2</sub>-QA)( $\eta^3$ -allyl)] **2**, with IC<sub>50</sub> of 360  $\pm$  2 and 531  $\pm$  8 nM, respectively. To compare the deallylation efficiency of [CpRu<sup>IV</sup>(NMe<sub>2</sub>-QA)( $\eta^3$ -allyl)] **2** and [CpRu<sup>IV</sup>(HQ)( $\eta^3$ -allyl)] **3** in the presence of CT26 cells, we used the alloc-gemcitabine **12** previously described by Mao and co-workers.<sup>27</sup> Firstly, the cytotoxicity of gemcitabine **13** and its caged analog **12** was determined. Gemcitabine **13** was about 500 times more toxic than alloc-gemcitabine **12**, with IC<sub>50</sub> of 12.1  $\pm$  0.2 nM and 5.86  $\pm$  0.05  $\mu$ M, respectively, Figure

9b. Next, we incubated CT26 cells with 1  $\mu\text{M}$  of alloc-gemcitabine **12**, whereby no cytotoxicity of alloc-gemcitabine **12** was observed. Then, the CT26 cells were treated with increasing concentrations of either  $[\text{CpRu}^{\text{IV}}(\text{NMe}_2\text{-QA})(\eta^3\text{-allyl})]$  **2** and  $[\text{CpRu}^{\text{IV}}(\text{HQ})(\eta^3\text{-allyl})]$  **3**, in the presence of 1  $\mu\text{M}$  alloc-gemcitabine **12**, Figure 9c. To minimize the cytotoxicity effect of the  $[\text{CpRu}^{\text{IV}}(\text{NMe}_2\text{-QA})(\eta^3\text{-allyl})]$  **2** and  $[\text{CpRu}^{\text{IV}}(\text{HQ})(\eta^3\text{-allyl})]$  **3**, their concentration was kept below 100 nM. As can be appreciated in Figure 9d, the catalytic activity of  $[\text{CpRu}^{\text{IV}}(\text{NMe}_2\text{-QA})(\eta^3\text{-allyl})]$  **2** and  $[\text{CpRu}^{\text{IV}}(\text{HQ})(\eta^3\text{-allyl})]$  **3** are comparable. A significant reduction in cell viability was only observed at a catalyst concentration  $>50$  nM for both catalysts. At a catalyst concentration of 100 nM, corresponding to a 10% catalyst loading, the cell viability was reduced to 64% and 56% for  $[\text{CpRu}^{\text{IV}}(\text{NMe}_2\text{-QA})(\eta^3\text{-allyl})]$  **2** and  $[\text{CpRu}^{\text{IV}}(\text{HQ})(\eta^3\text{-allyl})]$  **3**, respectively. Inspection of Figure 9a reveals that such a reduction of cell viability corresponds to a concentration of gemcitabine **13** in the 10 nM range. Under these experimental conditions ([substrate **12**] = 1 mM, [Ru(IV) catalyst **2** or **3**] = 100 nM, [product **13**] = 10 nM), we conclude that the conversion is roughly 1%, which corresponds to a TON = 0.1. However, we cannot exclude at this stage that the cytotoxicity observed in this assay results from a synergistic combination of the individual cytotoxic effects of the prodrug **12**, gemcitabine **13** and the  $[\text{CpRu}^{\text{IV}}(\text{NMe}_2\text{-QA})(\eta^3\text{-allyl})]$  **2** and  $[\text{CpRu}^{\text{IV}}(\text{HQ})(\eta^3\text{-allyl})]$  **3** and a perturbation of the GSH/GSSG ratio.

These control experiments reveal that, while analogs of  $[\text{CpRu}^{\text{IV}}(\text{HQ})(\eta^3\text{-allyl})]$  **3** have been reported to be more efficient than analogs of  $[\text{CpRu}^{\text{IV}}(\text{NMe}_2\text{-QA})(\eta^3\text{-allyl})]$  **2** *in vitro*, significant improvement of the catalytic activity in biological media is required before they can be considered safe for clinical applications in medicine.

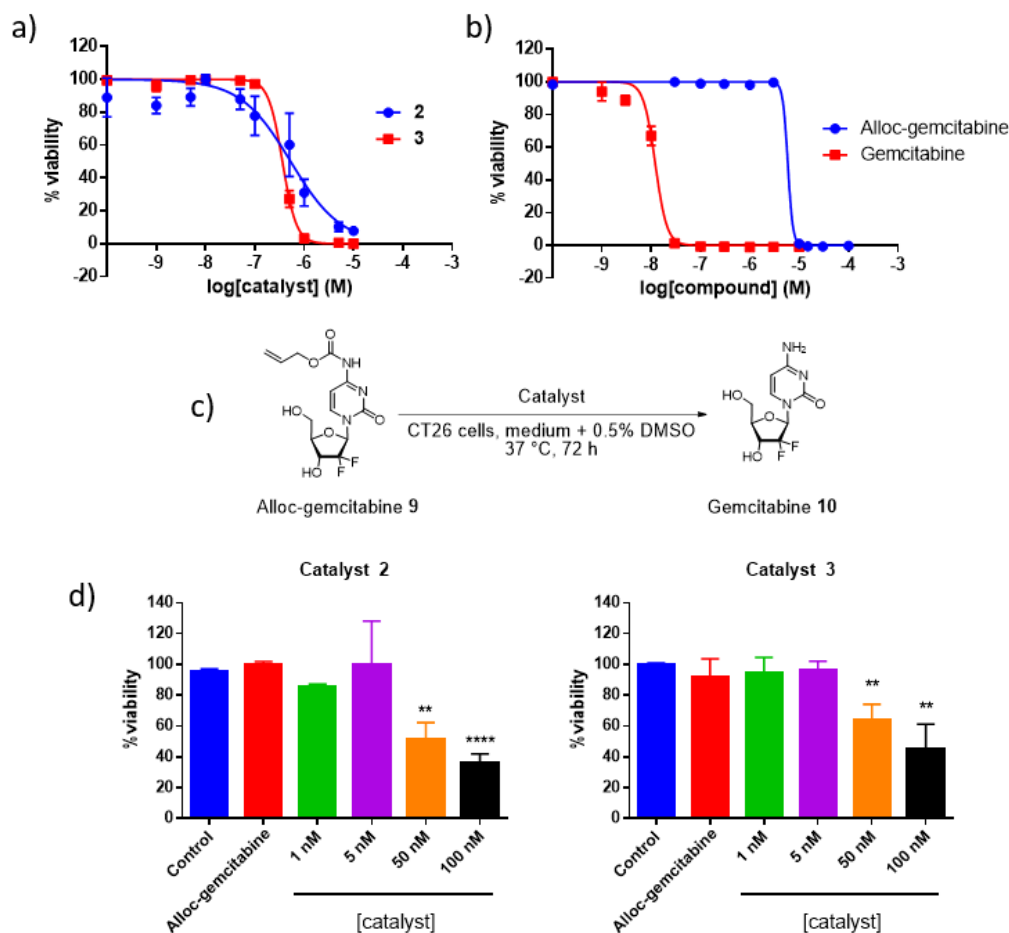


**Figure 9:** CT26 cell viability assays in the presence of alloc-gemcitabine **12**, [CpRu<sup>IV</sup>(NMe<sub>2</sub>-QA)(η<sup>3</sup>-allyl)] **2** or [CpRu<sup>IV</sup>(HQ)(η<sup>3</sup>-allyl)] **3** and gemcitabine **13** with 0.5 % DMSO. a) CT26 cells viability following 72 h incubation with either catalyst **2** or **3**. b) CT26 cells viability following 72 h of incubation with alloc-gemcitabine **12** or gemcitabine **13**. c) Deallylation of caged-gemcitabine **12** to gemcitabine **13**, catalyzed by catalyst **2** (left panel) or **3** (right panel). d) CT26 cells viability following 72 h incubation with 1 μM of alloc-gemcitabine **12** and increasing concentrations of catalyst **2** or **3**. \*\*\*\* P < 0.0001, \*\* P < 0.01 (unpaired t-test).

### 3.3 Conclusions

Ever since their initial report by Meggers in 2006, the CpRu deallylation catalysts have been widely investigated for biological applications. Over the years, the system has revealed some of its limitations, including i) catalyst deactivation by dioxygen, ii) undesirable allylation of the uncaged amine-moiety present in the product iii) thiol

oxidation, iv) high substrate dependency, and v) limited catalytic activity *in cellulo*. Although rather qualitative, this study reveals that the catalysts **1-3** are affected by the presence of both oxygen and thiols. Importantly, the co-solvent plays an important role on the stability of catalyst **1-3**. A complex kinetic interplay between glutathione oxidation and nucleophilic attack on the  $\eta^3$ -allyl group is presented. Future work in the group will explore the relation between substrate complexity and catalytic outcome, which we believe to be critical. While the *in cellulo* applications of these catalysts remain limited, they significantly contribute to coming-of-age using the cell as a “test-tube”. We believe that a thorough understanding of the mechanism and the associated side reactions will eventually enable the field to reach its maturity.

## References

- (1) Streu, C.; Meggers, E. Ruthenium-Induced Allylcarbamate Cleavage in Living Cells. *Angew. Chem., Int. Ed.* **2006**, *45* (34), 5645–5648. <https://doi.org/10.1002/anie.200601752>.
- (2) Völker, T.; Dempwolff, F.; Graumann, P. L.; Meggers, E. Progress towards Bioorthogonal Catalysis with Organometallic Compounds. *Angew. Chem., Int. Ed. Engl.* **2014**, *53* (39), 10536–10540. <https://doi.org/10.1002/anie.201404547>.
- (3) Tanaka, S.; Saburi, H.; Hirakawa, T.; Seki, T.; Kitamura, M. Dehydrative Allylation of Alcohols and Deallylation of Allyl Ethers Catalyzed by [CpRu(CH<sub>3</sub>CN)<sub>3</sub>]PF<sub>6</sub> and 2-Pyridinecarboxylic Acid Derivatives. Effect of  $\pi$ -Accepting Ability and COOH Acidity of Ligand on Reactivity. *Chem Lett* **2009**, *38* (2), 188–189. <https://doi.org/10.1246/cl.2009.188>.
- (4) Sánchez, M. I.; Penas, C.; Vázquez, M. E.; Mascareñas, J. L. Metal-Catalyzed Uncaging of DNA-Binding Agents in Living Cells. *Chem Sci* **2014**, *5* (5), 1901–1907. <https://doi.org/10.1039/c3sc53317d>.
- (5) Vornholt, T.; Christoffel, F.; Pellizzoni, M. M.; Panke, S.; Ward, T. R.; Jeschek, M. Systematic Engineering of Artificial Metalloenzymes for New-to-Nature Reactions. *Sci Adv* **2021**, *7* (4), eabe4208. <https://doi.org/10.1126/sciadv.abe4208>.
- (6) Völker, T.; Meggers, E. Chemical Activation in Blood Serum and Human Cell Culture: Improved Ruthenium Complex for Catalytic Uncaging of Alloc-Protected Amines. *ChemBioChem* **2017**, *18* (12), 1083–1086. <https://doi.org/10.1002/cbic.201700168>.
- (7) Tomás-Gamasa, M.; Martínez-Calvo, M.; Couceiro, J. R.; Mascareñas, J. L. Transition Metal Catalysis in the Mitochondria of Living Cells. *Nat Commun* **2016**, *7*, 12538. <https://doi.org/10.1038/ncomms12538>.

- (8) Vidal, C.; Tomás-Gamasa, M.; Destito, P.; López, F.; Mascareñas, J. L. Concurrent and Orthogonal Gold(I) and Ruthenium(II) Catalysis inside Living Cells. *Nat Commun* **2018**, *9* (1), 1913. <https://doi.org/10.1038/s41467-018-04314-5>.
- (9) Lohner, P.; Zmyslia, M.; Thurn, J.; Pape, J. K.; Gerasimaitė, R.; Keller-Findeisen, J.; Groer, S.; Deuringer, B.; Süß, R.; Walther, A.; Hell, S. W.; Lukinavičius, G.; Hugel, T.; Jessen-Trefzer, C. Inside a Shell—Organometallic Catalysis Inside Encapsulin Nanoreactors. *Angew. Chem., Int. Ed.* **2021**, *60* (44), 23835–23841. <https://doi.org/10.1002/anie.202110327>.
- (10) Ahmadi, P.; Muguruma, K.; Chang, T. C.; Tamura, S.; Tsubokura, K.; Egawa, Y.; Suzuki, T.; Dohmae, N.; Nakao, Y.; Tanaka, K. In Vivometal-Catalyzed SeCT Therapy by a Proapoptotic Peptide. *Chem Sci* **2021**, *12* (37), 12266–12273. <https://doi.org/10.1039/d1sc01784e>.
- (11) Cheng, Y.; Zong, L.; López-Andarias, J.; Bartolami, E.; Okamoto, Y.; Ward, T. R.; Sakai, N.; Matile, S. Cell-Penetrating Dynamic-Covalent Benzopolysulfane Networks. *Angewandte Chemie - International Edition* **2019**, *58* (28), 9522–9526. <https://doi.org/10.1002/anie.201905003>.
- (12) Okamoto, Y.; Kojima, R.; Schwizer, F.; Bartolami, E.; Heinisch, T.; Matile, S.; Fussenegger, M.; Ward, T. R. A Cell-Penetrating Artificial Metalloenzyme Regulates a Gene Switch in a Designer Mammalian Cell. *Nat Commun* **2018**, *9*, 1943 (1). <https://doi.org/10.1038/s41467-018-04440-0>.
- (13) Jaisankar, P.; Tanaka, S.; Kitamura, M. Catalytic Dehydrative S-Allylation of Cysteine-Containing Peptides in Aqueous Media toward Lipopeptide Chemistry. *Journal of Organic Chemistry* **2011**, *76* (6), 1894–1897. <https://doi.org/10.1021/jo102278m>.
- (14) Tanaka, S.; Pradhan, P. K.; Maegawa, Y.; Kitamura, M. Highly Efficient Catalytic Dehydrative S-Allylation of Thiols and Thioic S-Acids. *Chem. Commun.* **2010**, *46* (22), 3996–3998. <https://doi.org/10.1039/c0cc00096e>.
- (15) Kiesewetter, M. K.; Waymouth, R. M. Kinetics of an Air- and Water-Stable Ruthenium(IV) Catalyst for the Deprotection of Allyl Alcohol in Water. *Organometallics* **2010**, *29* (22), 6051–6056. <https://doi.org/10.1021/om100892v>.
- (16) Hsu, H. T.; Trantow, B. M.; Waymouth, R. M.; Wender, P. A. Bioorthogonal Catalysis: A General Method to Evaluate Metal-Catalyzed Reactions in Real Time in Living Systems Using a Cellular Luciferase Reporter System. *Bioconjug Chem* **2016**, *27* (2), 376–382. <https://doi.org/10.1021/acs.bioconjchem.5b00469>.
- (17) Rubini, R.; Ivanov, I.; Mayer, C. A Screening Platform to Identify and Tailor Biocompatible Small-Molecule Catalysts. *Chem. - Eur. J.* **2019**, *25* (70), 16017–16021. <https://doi.org/10.1002/chem.201904808>.
- (18) Mancuso, F.; Rahm, M.; Dzijak, R.; Mertlíková-Kaiserová, H.; Vrabel, M. Transition-Metal-Mediated versus Tetrazine-Triggered Bioorthogonal Release Reactions: Direct Comparison and Combinations Thereof. *Chempluschem* **2020**, *85* (8), 1669–1675. <https://doi.org/10.1002/cplu.202000477>.
- (19) Southwell, J.; Herman, R.; Raines, D.; Clarke, J.; Boeswald, I.; Dreher, T.; Gutenthaler, S.; Schubert, N.; Seefeldt, J.; Metzler-Nolte, N.; Thomas, G.; Wilson, K.; Duhme-Klair, A.-K. Siderophore-linked Ruthenium Catalysts for Targeted Allyl Ester Prodrug Activation within Bacterial Cells. *Chem. - Eur. J.* **2022**. <https://doi.org/10.1002/chem.202202536>.

- (20) Mascarenas, J. L.; Gutierrez-González, A.; López, F. Ruthenium Catalysis in Biological Habitats. *Helv Chim Acta* **2023**. <https://doi.org/10.1002/hlca.202300001>.
- (21) Franco, R.; Cidlowski, J. A. Apoptosis and Glutathione: Beyond an Antioxidant. *Cell Death Differ.* 2009, pp 1303–1314. <https://doi.org/10.1038/cdd.2009.107>.
- (22) Homer, N. Z. M.; Reglinski, J.; Sowden, R.; Spickett, C. M.; Wilson, R.; Walker, J. J. Dimethylsulfoxide Oxidizes Glutathione in Vitro and in Human Erythrocytes: Kinetic Analysis by <sup>1</sup>H NMR. *Cryobiology* **2005**, *50* (3), 317–324. <https://doi.org/10.1016/j.cryobiol.2005.04.002>.
- (23) Takenaka, M.; Kikkawa, M.; Matsumoto, T.; Yatabe, T.; Ando, T.; Yoon, K. S.; Ogo, S. Oxidation of Guanosine Monophosphate with O<sub>2</sub> via a Ru-Peroxo Complex in Water. *Chem. - Asian J.* **2018**, *13* (21), 3180–3184. <https://doi.org/10.1002/asia.201801267>.
- (24) Albertin, G.; Antoniutti, S.; Bortoluzzi, M.; Castro, J.; Ferraro, V. Preparation and Reactivity of Half-Sandwich Dioxygen Complexes of Ruthenium. *Dalton Trans.* **2018**, *47* (27), 9173–9184. <https://doi.org/10.1039/c8dt01871e>.
- (25) Ishizuka, T.; Sugimoto, H.; Itoh, S.; Kojima, T. Recent Progress in Oxidation Chemistry of High-Valent Ruthenium-Oxo and Osmium-Oxo Complexes and Related Species. *Coord. Chem. Rev.* Elsevier B.V. September 1, **2022**. <https://doi.org/10.1016/j.ccr.2022.214536>.
- (26) Seki, T.; Tanaka, S.; Kitamura, M. Enantioselective Synthesis of Pyrrolidine-, Piperidine-, and Azepane-Type N -Heterocycles with  $\alpha$ -Alkenyl Substitution: The CpRu-Catalyzed Dehydrative Intramolecular N -Allylation Approach. *Org Lett* **2012**, *14* (2), 608–611. <https://doi.org/10.1021/ol203218d>.
- (27) Zhao, Z.; Tao, X.; Xie, Y.; Lai, Q.; Lin, W.; Lu, K.; Wang, J.; Xia, W.; Mao, Z. W. In Situ Prodrug Activation by an Affibody-Ruthenium Catalyst Hybrid for HER2-Targeted Chemotherapy. *Angew. Chem., Int. Ed.* **2022**, *61* (26). <https://doi.org/10.1002/anie.202202855>.